JOURNAL OF EXPERIMENTAL ZOOLOGY 293:561–577 (2002)

Mechanical Properties of the Dorsal Fin Muscle of Seahorse (*Hippocampus*) and Pipefish (*Syngnathus*)

MIRIAM A. ASHLEY-ROSS*
Department of Biology, Wake Forest University, Winston-Salem, North Carolina 27109

ABSTRACT The dorsal and pectoral fins are the primary locomotor organs in seahorses (*Hippocampus*) and pipefish (*Syngnathus*). The small dorsal fins beat at high oscillatory frequencies against the viscous medium of water. Both species are able to oscillate their fins at frequencies likely exceeding the point of flicker fusion for their predators, thus enhancing their ability to remain cryptic. High-speed video demonstrated that seahorse dorsal fins beat at 30–42 Hz, while pipefish dorsal fins oscillate at 13–26 Hz. In both species, the movement of the fin is a sinusoidal wave that travels down the fin from anterior to posterior. Mechanical properties of seahorse and pipefish dorsal fin muscles were tested in vitro by the work loop method. Maximum isometric stress was 176.1 kN/m^2 in seahorse and 111.5 kN/m^2 in pipefish. Work and power output were examined at a series of frequencies encompassing the range observed in vivo, and at a number of strains (percent length change during a contractile cycle) within each frequency. At a given strain, work per cycle declined with increasing frequency, while power output rose to a maximum at an intermediate frequency and then declined. Frequency and strain interacted in a complex fashion; optimal strain was inversely related to cycle frequency over most of the frequency range tested. Seahorse dorsal fin muscle was able to generate positive work at higher cycling frequencies than pipefish. Both species produced positive work at higher frequencies than have been reported for axial and fin muscles from other fish. *J. Exp. Zool. 293:561–577, 2002.* © 2002 Wiley-Liss, Inc.

Locomotion via movements of the median fins has arisen independently multiple times in the evolution of fishes. The methods of median fin propulsion are as varied as the taxa that employ them (reviewed in Lindsey, '78). Locomotion by dorsal fin undulation is classified as amiiform (exemplified by *Amia calva*, but also seen in many mormyrids, *Gymnarchus*, and syngnathids, including *Syngnathus* and *Hippocampus*). Gymnotiform locomotion is characterized by undulations of the anal fin only (seen in gymnotids and notopterids). Undulation of both dorsal and anal fins is referred to as balistiform (seen in triggerfish and their relatives, some cichlids, centriscids, and flatfish). Finally, tetraodontiform locomotion is defined as oscillations of short-based dorsal and anal fins (seen in pufferfish and ostraciids). Median fin propulsion is associated with relatively slow, but precise, locomotion in complex habitats such as coral reefs and obstacle-strewn stream or sea beds (Lindsey, '78; Webb, '82; Videler, '93). Most fish that use median fin propulsion generate low-frequency waves ($\approx$2 Hz) of high amplitude in the fins, allowing them to swim with high hydrodynamic efficiency (defined as useful power output divided by power input to move the fin; Blake, '80). The family Syngnathidae, comprising the seahorses and pipefish, is an exception: Members of this group undulate their dorsal fins at very high frequencies ($>$40 Hz in seahorses; Breder and Edgerton, '42; Blake, '76) with low amplitude, leading to reduced efficiency and very slow swimming speeds (Blake, '80).

Because the swimming speeds of seahorses and pipefish are slow, one may expect that the musculature powering dorsal fin movements would be relatively weak. However, the dorsal fin muscle is required to contract against substantial resistance as it beats the fin back and forth through the viscous medium of water. Furthermore, the muscle must contract at a high frequency while performing positive work against the environment. Indeed, the oscillation is so rapid

Grant sponsor: Grass Foundation (Grass Fellowship in Neurophysiology at Woods Hole); Grant sponsor: National Science Foundation; Grant number: IBN-9813730.

*Correspondence to: Miriam A. Ashley-Ross, Department of Biology, Box 7325, Wake Forest University, Winston-Salem, NC 27109. E-mail: rossma@wfu.edu

Received 16 November 2001; Accepted 22 May 2002
Published online in Wiley InterScience (www.interscience.wiley.com). DOI: 10.1002/jez.10183

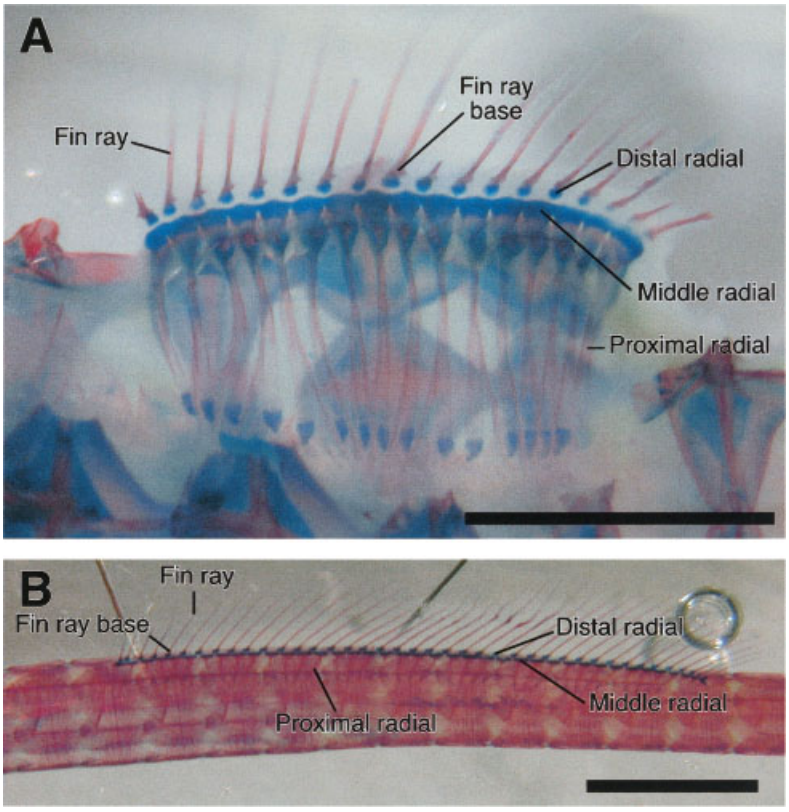

Fig. 1. Cleared and stained specimens of *H. hudsonius* (**A**) and *S. fuscus* (**B**) showing the skeletal supports of the dorsal fin. Surface scales of *S. fuscus* over the proximal radials have not been removed; proximal radials are visible through the translucent scales. Bone appears red, cartilage appears blue. The dorsal fin consists of a series of 16–20 bony rays connected by a flexible membrane. The fin ray bases are supported by a series of midline skeletal elements radiating dorsally from the vertebral column; in order, these are the proximal radials, middle radials, and distal radials, followed by the fin ray base itself. The proximal radials are bony, while the middle and distal radials are cartilaginous. The middle radials are fused together into a rigid beam-like structure in the seahorse; in pipefish, the middle radials do not form a single continuous structure, but individual middle radials are bound together by connective tissue. Scale bars in both panels are 0.5 cm.

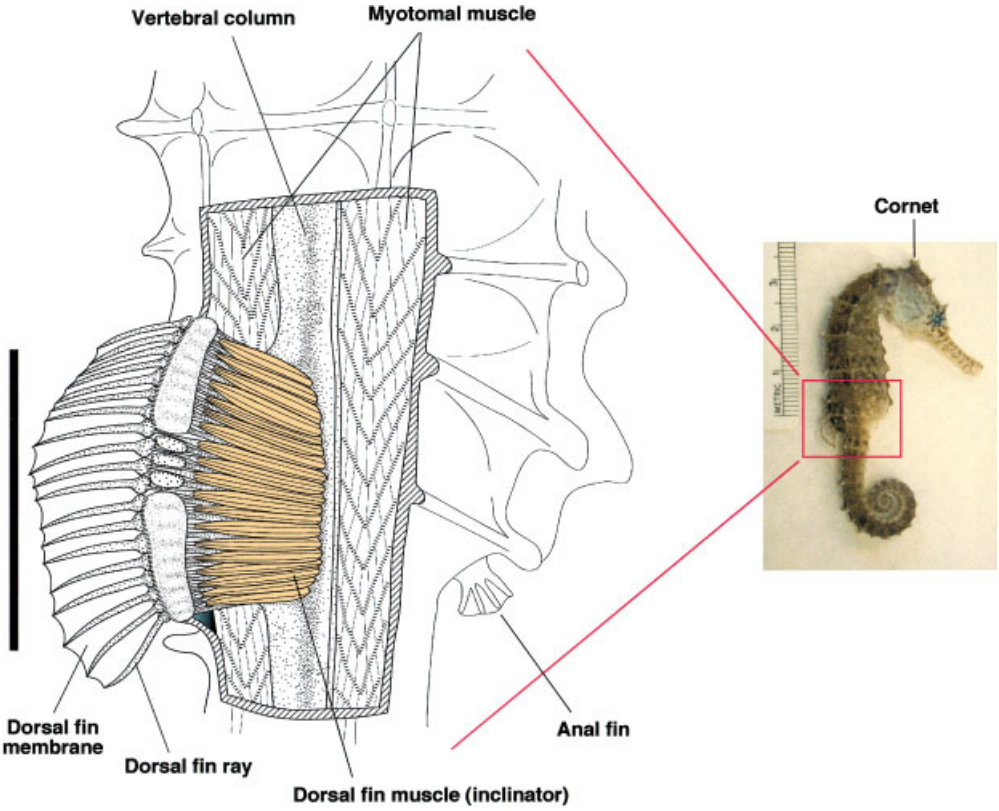

Fig. 2. Anatomy of the dorsal fin muscle in the seahorse, *Hippocampus*. The box over the seahorse on the right side of the figure indicates the area that is enlarged on the left side of the figure. Muscle is colored yellow. The dorsal fin muscle consists of a layer of inclinator muscle slips and a layer of depressor muscle slips. The inclinator muscles arise from the lateral processes of the vertebrae and insert via a narrow tendon onto the fin ray base at approximately the midpoint of the distal radial upon which the fin ray base rides. The depressor muscles resemble the inclinator muscles in appearance; they are located deep to the inclinators, arise from the vertebrae, and narrow to long tendons that insert on the posterolateral fin ray base. For clarity, only the inclinator muscles are shown. Anatomy of the dorsal fin and its associated muscle is similar in the pipefish. Scale bar, 1 cm.

that it exceeds the flicker fusion frequency of the human eye, and likely those of predators as well (Blake, '76). The dorsal fin is thus rendered effectively invisible as it propels the animal.

In vertebrates, high frequency muscles are associated with at least three activities: sound production, eye movements, and locomotion. Sound producing and ocular positioning muscles tend to have the faster contraction times. In the sound producing group are the bat cricothyroid muscle, the midshipman sonic muscle, the toadfish sonic muscle (all with in vivo contraction frequencies ≥ 100 Hz; Fawcett and Revel, '61; Revel, '62; Fine, '89; Bass and Marchaterre, '89; Bass, '90; Fine et al., '90; Rome et al., '96, '99, respectively), and rattlesnake shaker muscle (contraction frequency ≈ 50 Hz; Clark and Schultz, '80; Schultz et al., '80). These muscles are all thought to contract nearly isometrically and to do little mechanical work in vivo. Likewise, muscles responsible for eye movements have very fast contraction times (< 10 ms), but produce little force, and hence small amounts of mechanical work (Cooper and Eccles, '30; Close and Luff, '74).

In contrast, fast locomotory muscles, such as hummingbird pectoral muscle (30–78 Hz; Greenewalt, '75) and sea horse dorsal fin muscle (> 30 Hz; Breder and Edgerton, '42), tend to have lower frequencies of contraction. However, these muscles must produce mechanical work and power if they are to propel their bearer about. Hummingbird pectoral muscles are responsible for producing sufficient power to allow sustained hovering, one of the most energetically expensive locomotor activities (Suarez et al., '91; Withers, '92). Assuming a Q_{10} value of 2, when brought to the same temperature the contraction frequency of the dorsal fin musculature of the sea horse would be similar to that of hummingbird pectoral muscle.

Seahorse locomotion has been previously studied from the standpoint of anatomy of the locomotor apparatus (Consi et al., 2001), kinematics using high-speed video (Breder and Edgerton, '42; Blake, '76), and hydrodynamic theory (Blake, '76). Consi et al. (2001) described in detail the anatomy of the dorsal fin of seahorses, including the joints between skeletal elements of the fin (Fig. 1). Transverse movements of the fin ray are allowed at the joint between the middle and distal radials (with the fin ray base riding passively on the distal radial), while longitudinal movements of the fin ray (elevation and depression) occur at the joint between the fin ray base and the distal radial (Consi et al., 2001). Two muscles move each individual fin ray on either side of the animal: an inclinator muscle and a depressor muscle (collectively referred to as the dorsal fin muscle; Fig. 2). The inclinator muscles of seahorses and pipefish are likely derived from the dorsal fin elevator muscles of more typical fish (Winterbottom, '74; Geerlink and Videler, '74; Consi et al., 2001).

Properties of the dorsal fin muscle of seahorses have been investigated by examination of subcellular anatomy and isometric properties. Published ultrastructural studies of sea horse dorsal fin muscle have demonstrated polyneuronal innervation similar to other fish muscles (Smith et al., '88), large numbers of mitochondria (making up to 10% of a muscle cell's volume; Smith et al., '88), and an extensive sarcoplasmic reticulum (occupying approximately 28% of the fiber volume; Bergman, '64b; Smith et al., '88) similar to that of other fast muscles. The sarcoplasmic reticulum shows a highly ordered distribution within the cell, with triads situated at the Z lines (Smith et al., '88). Dorsal fin muscle also shows an exceptionally high ratio of sarcoplasm volume to myofibril volume (Bergman, '64b). Investigation of the contractile capabilities of the dorsal fin muscle of *Hippocampus hudsonius* has thus far been limited to measurements of twitch contraction time and fusion frequency (Bergman, '64a). No studies have yet addressed the mechanical properties of the dorsal fin muscle under conditions resembling those in vivo. Therefore, the goal of this study was to characterize the work and power output capabilities of the dorsal fin muscle of the seahorse, *Hippocampus*, and its close relative, the pipefish, *Syngnathus*, as a first step in understanding the changes in muscle composition that must have occurred in the evolution of these specialized, high-frequency dorsal fin muscles.

MATERIALS AND METHODS

Animals

Northern pipefish, *Syngnathus fuscus* (12.6–18.8 cm standard length), were obtained from the Marine Resources department of the Marine Biological Laboratory at Woods Hole, MA. They were maintained in 80 l tanks with flow-through seawater and fed adult brine shrimp several times per day.

Two species of seahorses, *Hippocampus hudsonius* and *H. zosterae,* were obtained through the aquarium trade, primarily from Florida-based

vendors. Specimens of *H. hudsonius* ranged in size from 14.9–16.5 cm standard length which, due to the unusual body posture of seahorses, was calculated as the sum of two measurements: the distance from the tip of the snout to the posterior side of the base of the cornet, and the distance from the posterior side of the base of the cornet (see Fig. 2) to the tip of the uncurled tail. Dwarf seahorses, *H. zosterae,* were 2.4–3.3 cm standard length. Seahorses were kept either in 80 l tanks with flow-through seawater (all *H. zosterae*, some *H. hudsonius*) or in 40 l aquaria filled with artificial seawater (Instant Ocean; some *H. hudsonius*). Seahorses were fed a mixture of adult brine shrimp and ghost shrimp (*H. hudsonius* only) several times per day. All fish, both seahorses and pipefish, were used for experiments within one week of arrival in the laboratory.

High-speed video of fin movements

Fin movements of pipefish and seahorses were videotaped at 500 frames/sec using a Kodak Ektapro EM1000 high-speed video system equipped with a zoom lens. As none of the species involved naturally maintains steady swimming, sequences were recorded as the fish moved freely in aquaria. Only periods of steady fin movement were sampled, and 3–13 fin beat cycles were recorded for each individual. Two *H. hudsonius*, two *H. zosterae*, and four *S. fuscus* were videotaped. Fin beat frequencies were calculated from the videos.

In vitro measures of work and power output

Only *S. fuscus* and *H. hudsonius* were used for in vitro work, as *H. zosterae* dorsal fin muscles proved inconveniently small. Fish were first anesthetized by immersion in a solution of tricaine methane sulfonate (MS-222; 1.5 g/l) prepared in seawater or artificial seawater until the righting reflex disappeared. Fish were then decapitated and the rest of the body was cut away from the section containing the dorsal fin. The abdominal wall (skin and musculature) was cut away, and the internal organs in this region were removed, leaving the dorsal portion of the body containing the dorsal fin, vertebral column, epaxial musculature, and the bony plates. This remaining section of the body was then placed in a dissecting dish under Ringer's solution. The Ringer's solution contained, in mM: NaCl 145, KCl 4, $CaCl_2$ 2.4, $MgSO_4$ 1.7, $MgCl_2$ 1.5, Na_2HPO_4 2.5, KH_2PO_4 0.4, D-glucose 10, HEPES 10. pH was adjusted to 7.6 at 20°C with KOH (Knapp and Dowling, '87). The rest of the preparation was carried out under a dissecting microscope. The section was pinned to the bottom of the dissecting dish so that the dorsal fin pointed up, and incisions were made with a scalpel on either side of the dorsal fin through the bony plates, taking care not to cut into the underlying muscle too deeply. Cuts were made with scissors through the bony plates on the sides of the section, just dorsal to the lateral processes of the vertebrae. Then the bony ''exoskeleton'' was deflected laterally with forceps, and the myotomal muscle was cut away from the connective tissue overlying the dorsal fin muscle, eventually freeing the dorsolateral portion of the body section to be entirely discarded. The remaining part of the preparation was composed of the dorsal fin, vertebral column, and the dorsal fin muscle on both sides of the vertebral column. The sheet of connective tissue that overlies the dorsal fin muscle was carefully removed, finally exposing the dorsal fin muscle, which is composed of a series of parallel slips of inclinators and depressors connected by tendons to the bases of the dorsal fin rays (Fig. 2). Next, the dorsal fin muscle on one side of the body was completely removed, exposing the proximal radials that support the dorsal fin. Very fine-tipped spring scissors were used to carefully cut through the proximal radials, thus freeing the ends of the muscle slips to move relative to one another without the bony strut between them (which normally turns the linear contraction of the dorsal fin muscle into lateral movement of the dorsal fin rays; see Fig. 3A). The muscle slips were examined for any damage, and a series of 4–6 intact slips (composed of both inclinators and depressors) were selected, always near the middle of the dorsal fin. This series of slips, together with the associated fin rays and section of vertebral column, was cut away from the surrounding tissues and transferred into a Plexiglas experimental chamber containing 40 ml of Ringer's solution. Chamber temperature was maintained at 20°C by a water bath circulating fluid through a channel surrounding the experimental chamber. The Ringer's solution was aerated throughout the experiment. The lateral processes of the vertebrae on the side opposite the dorsal fin muscle were fixed in a clamp at the bottom of the chamber, and the fin rays were gathered together and tied with silk suture onto the arm of a servomotor ergometer (Cambridge Technology, Cambridge, MA and Aurora Scientific, Ontario, Canada; model 300B) that also

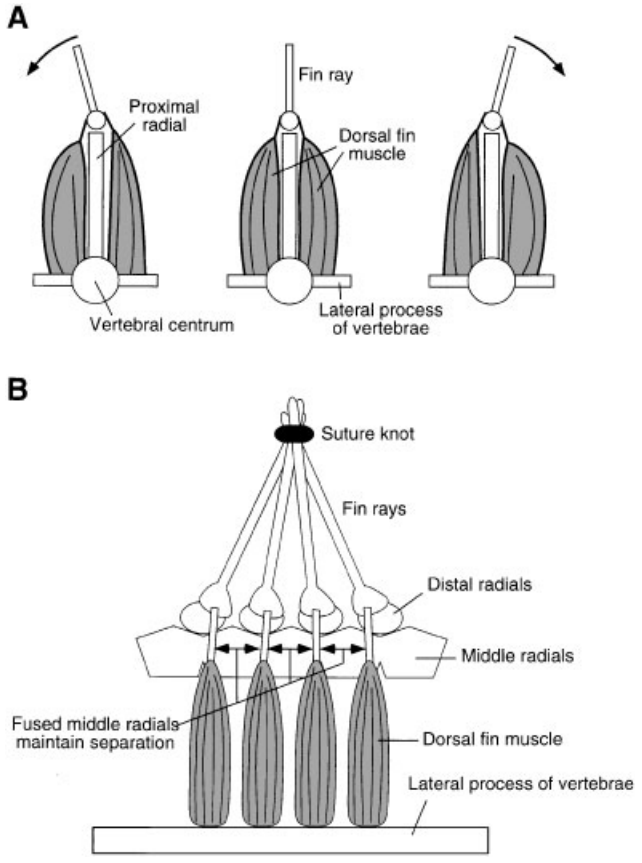

Fig. 3. **A:** Schematic of how the dorsal fin inclinator muscles work. The figure depicts a cross-section of the vertebral column. Fin muscles on either side of the vertebral column alternately contract, pulling the fin ray first to one side, then the other. A traveling wave passes down the fin due to a phase lag in the fin ray movements from anterior to posterior. **B:** Schematic of how the fused middle radials function as a rigid beam to maintain separation between the fin rays and fin ray muscles in the experimental setup.

functioned as a force transducer. One advantage of the arrangement of the dorsal fin structures is that the middle radials, which articulate with the distal radials and fin ray bases, are fused or bound together to form a rigid beam, which permits the contribution of multiple muscle slips to be measured without introducing potential complications of the outside slips contracting at an angle to the inner slips (see Fig. 3B).

The muscle was stimulated using a Grass S88 or S8800 stimulator connected to silver plate electrodes that were placed in the bath on either side of the muscle. Force and position, both sensed by the ergometer, were recorded using a custom-written computer program that also triggered the stimulator. Muscle length, stimulus strength, and stimulus frequency were adjusted to produce maximal isometric tetanic force. Typical values for stimulation frequency necessary to produce fused tetani were 100–120 Hz, at a voltage intensity of 80 V through the bath electrodes. Maximal twitch and tetanic force were recorded, and the muscle length (L_o) was measured through a dissecting microscope. Mechanical work and power output was measured using the work loop method (Josephson, '85), in which the muscle was subjected to symmetrical sinusoidal length changes while being stimulated phasically during the length change cycle. Plotting muscle force versus length over a cycle of oscillation results in a loop-shaped trace. Because work is the product of force and distance, the area enclosed by the loop is the work performed by the muscle during that cycle. Mechanical work and power output (work per cycle times oscillation frequency) were measured at frequencies that encompassed the range of fin oscillation observed in the high-speed video recordings. For pipefish, the oscillation frequencies used were 5, 10, 15, 20, 25, and 30 Hz. For seahorses, frequencies were 20, 30, 40, and 50 Hz. Several different strains (peak-to-peak muscle length change as a percentage of L_o) were used. Pipefish were tested at strains of 2.5%, 5%, 10%, 15%, and 20% of L_o. Preliminary experiments on seahorse muscle demonstrated rapid deterioration of the muscle at 20% strain, so a more restricted range was used: 2.5%, 4%, 5%, 6%, 8%, 10%, 12%, and 15% of L_o. The phase and duration of the stimulus train were optimized to produce maximal work per cycle at each frequency+strain combination. The order in which frequencies were tested was random; however, the order in which strains were tested within each frequency was always from smallest to largest. This was done due to concern that the longest strains might cause damage to the muscle. The computer program generated a series of four consecutive length change cycles, and work per cycle was measured for cycle 3. Trials were separated by two minutes. Three measurements were made at each frequency+strain combination for each individual. The experiment was ended when isometric tension fell below 90% of the initial value. The Ringer's solution was changed and isometric tension was checked periodically during the experiment. Preparations were extremely stable, often lasting for 10–12 hours. Values for a particular frequency +strain combination represent the mean of data from 3–6 individuals. Temperature effects on muscle mechanics were examined in pipefish by testing four individuals at both 10°C and 20°C in

the following frequency+strain combinations: 5 Hz and 10 Hz; within each frequency, 2.5%, 5%, and 10% strain.

Following each experiment, the muscle was dissected away from the surrounding tissues and weighed to the nearest 0.1 mg. Cross-sectional area was calculated by converting mass to volume (assuming muscle density of 1.05 kg/m^3) and then dividing by L_o.

For each muscle, L_o, cross-sectional area, maximum isometric twitch and tetanic forces, time from stimulus to peak force (both twitch and tetanus), maximum isometric twitch and tetanic stress, mean work per cycle, and mean power output were determined. Data for the muscles from the two species were analyzed for statistical significance in StatView for Macintosh (version 5.0; SAS Institute, Cary, NC) using MANOVA for the isometric variables, and three-way ANOVAs for work and power output that considered species, oscillation frequency, and strain as the main effects. The three-way ANOVAs were conducted only on the frequencies and strains for which data was available for both seahorses and pipefish: 20 and 30 Hz, and 2.5%, 5%, 10%, and 15% strain. Temperature effects were analyzed by computing Q_{10} values and comparing work per cycle using a single factor ANOVA with temperature as the main effect. Differences were considered significant at $\alpha=0.05$.

RESULTS

High-speed video

Representative fin beat sequences from *S. fuscus* and *H. hudsonius* are shown in Fig. 4. These sequences, as well as additional movies of oscillating dorsal fins (including one of *H. zosterae*), are posted as QuickTime movies on the World Wide Web at http://www.wfu.edu/~rossma/finmovies.html. For pipefish, the oscillation frequencies observed in swimming animals were 13–26 Hz (mean 20.7 Hz). Multiple waves are present in the fin simultaneously (the wavelength is shorter than the fin; Fig. 4A). For *H. hudsonius*, fin beat frequencies during swimming were 30–42 Hz (mean 37.6 Hz). As in pipefish, the propulsive wavelength is shorter than the fin (Fig. 4B). Fin beat frequencies were higher in the dwarf seahorse, *H. zosterae*, ranging from 42–54 Hz (mean 47.4 Hz). Unlike the larger species examined, in the dwarf seahorses, only a single propulsive wave was visible in the fin at any given instant; in fact, the wavelength appeared to be substantially longer than the length of the fin (not shown, but see QuickTime movie). In all fin beat sequences observed for all species, oscillation of the fin either began along the entire length of the fin at once, or the oscillation began at the anterior end and progressed posteriorly until the entire fin was involved. Oscillation was never observed to begin in the posterior regions of the fin and spread to more anterior sites. Each individual fin ray beats side to side in a sinusoidal pattern (Fig. 4C); a phase lag between the rays such that each ray leads the one posterior to it generates the traveling wave pattern.

Isometric and anatomical measures

The series of slips of dorsal fin muscle removed from *H. hudsonius* and *S. fuscus* were similar in cross-sectional area, but differed in their resting length (L_o) and isometric force production (Table 1). MANOVA performed on the anatomical and isometric properties of the muscles from the two species demonstrated a significant multivariate difference between them (Wilk's $\lambda=0.104$, $F=17.284$, $P=0.0001$). All variables, except cross-sectional area (which was heavily influenced by the experimenter according to how many muscle slips were removed), were significantly different in post-hoc tests (Table 1). Resting length, twitch and tetanic stress were all higher in *H. hudsonius* than *S. fuscus*, while the rise times to maximum twitch and tetanic force were faster in *H. hudsonius* (Table 1). The faster rise times are correlated with the faster fin beat frequencies observed in seahorses (see above).

Representative twitch and tetanic contractions for seahorses and pipefish are shown in Fig. 5. In both species, the twitch record looks similar to that seen from other muscles. However, the tetanic traces always showed an unusual pattern in which the force would rise to an initial peak and then decline rapidly before stopping at a plateau of force (that was always higher than the twitch force) that was maintained throughout the stimulus period (Fig. 5). The decline of force from the tetanus plateau followed a slower timecourse than that seen in a twitch contraction (Fig. 5).

In vitro muscle mechanics

The cycling frequencies selected for each species completely overlapped the range of fin beat frequencies observed in swimming animals (see above). Only two frequencies (20 Hz and 30 Hz) were examined in both seahorses and pipefish, and

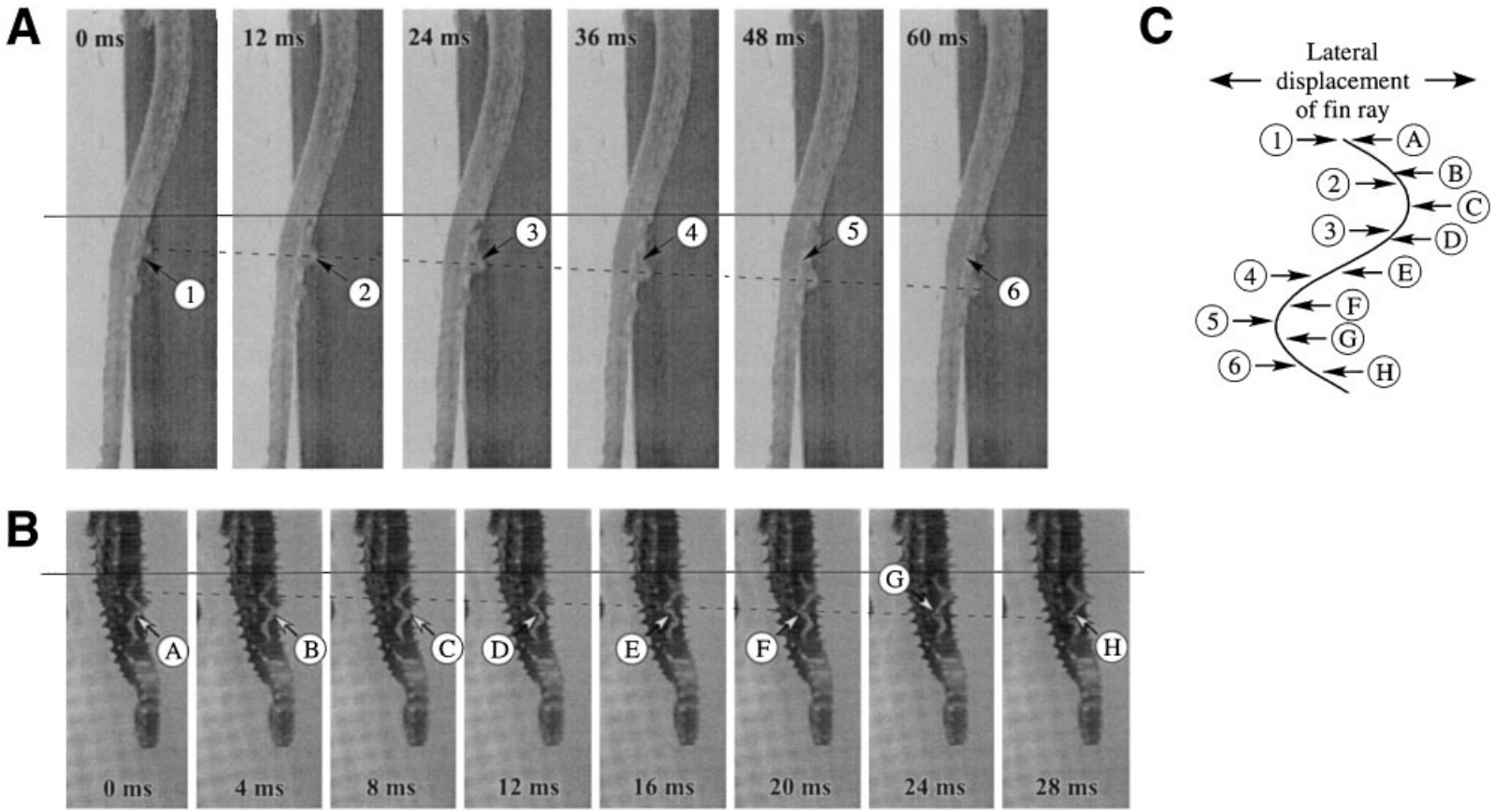

Fig. 4. Representative fin beat sequences recorded at 500 frames/sec. Individual frames have been cropped and composited using Canvas 7 (Deneba Systems, Inc., Miami, FL). **A:** Pipefish, *S. fuscus;* anterior is toward the top of the frames. **B:** Seahorse, *H. hudsonius;* anterior is toward the top. In both (A) and (B), the solid horizontal lines indicate the anterior edge of the dorsal fin, while the dashed lines connect the crest of a single propulsive wave as it moves posteriorly along the fin. A single fin beat cycle is shown in each sequence. **C:** Schematic indicating the pattern of side-to-side movement of a single fin ray. Numbers with arrows indicate the position of the fin ray at times during a single fin beat cycle and correspond to the numbered arrows in the panels of (A). Similarly, letters with arrows correspond to the frames of (B).

TABLE 1. Anatomical and isometric parameters for dorsal fin muscle of H. hudsonius and S. fuscus

	Hippocampus	Syngnathus	*P*-value
Cross-sectional area (mm^2)	2.89 (0.82)	2.64 (1.33)	ns
L_o (mm)	5.40 (1.20)	2.30 (0.44)	<0.0001
Max twitch stress (kN/m^2)	124 (53.3)	50 (23.9)	0.0008
Time to max twitch force (ms)[2]	19 (2.0)	22 (4.1)	0.0206
Max tetanic stress (kN/m^2)	176 (62.1)	112 (48.7)	0.0252
Time to max tetanic force (ms)[3]	25 (5.2)	36 (5.9)	0.0021

[1]Values are given as mean (SD). For all *Hippocampus* values, n=6; for *Syngnathus* values, n=13, except where otherwise noted.
[2]n=11
[3]n=10

work and power output at these frequencies were compared statistically. Representative work loops from several frequencies at 5% strain in both species are shown in Fig. 6. Individual work loops were selected because they were close to the mean work (in μJ) recorded for that frequency+strain combination. At the same strain, *Hippocampus* dorsal fin muscle is able to generate positive work at higher frequencies than that of *Syngnathus*.

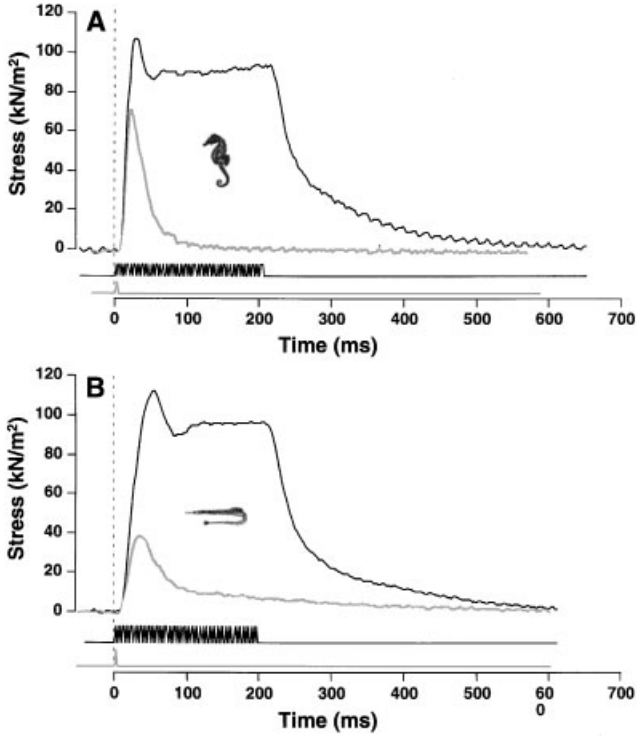

Fig. 5. Representative isometric twitch and tetanus from seahorse (**A**) and pipefish (**B**). Upper traces in each panel are force, lower traces are the stimulus monitor. Black traces depict tetanus, grey traces depict twitch contractions and stimulus.

Seahorse dorsal fin muscle performs positive work (albeit a small amount) at frequencies as high as 50 Hz, while pipefish dorsal fin muscle is no longer able to contract fast enough to keep up with the servomotor arm, and thus performs negative work (it is being lengthened by the servomotor during the time of maximum activation; Fig. 6). In both species, the phase of stimulation for maximal work production decreased (became earlier) as cycling frequency increased. Likewise, the duty factor (proportion of the cycle occupied by the stimulus) for maximal work production decreased as frequency increased (Fig. 6).

Mean values for work per cycle and power output of the dorsal fin muscle of *Hippocampus* and *Syngnathus* at different frequencies and strains are shown in Figs. 7 and 8, respectively. In general, work per cycle at a given strain declined with increasing frequency in both species (Fig. 7). At higher frequencies, the absolute time during which force can be developed and produce positive work is reduced, leading to a lower net work during a single contraction cycle. The effect of strain on work performed was more complicated and dependent upon the cycling frequency. At low frequencies, work per cycle increased as strain increased from the lowest value used (2.5% L_o) up to some optimum value, which was typically 6% in *Hippocampus* and 10% in *Syngnathus* (Figs. 7, 9). Increasing strain beyond this value resulted in a decrease in work per cycle and, in fact, would often result in negative work (Fig. 7). As the frequency of oscillation was increased, the value of muscle strain that resulted in maximum work decreased by a small increment in the seahorse, but very noticeably in the pipefish (Figs. 7, 9). Seahorse muscle was able to generate positive work at higher cycling frequencies than pipefish muscle (Fig. 7). Several trials of pipefish dorsal fin muscle at 40 Hz (not shown) resulted in negative work at

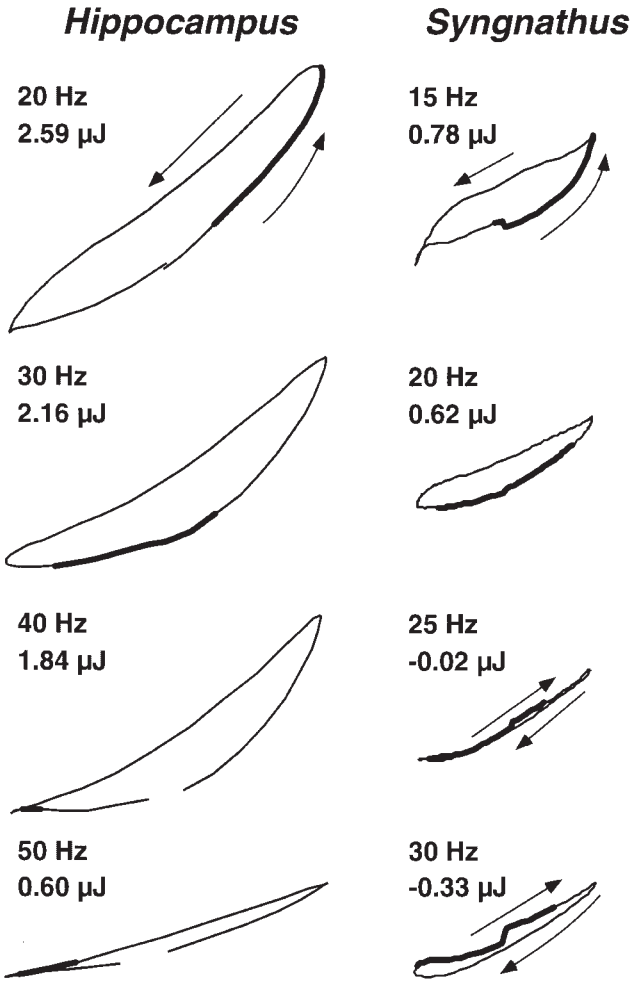

Fig. 6. Representative work loops at different cycling frequencies from the seahorse (left column) and pipefish (right column). Frequency and work recorded for the cycle shown is indicated in the upper left of each panel. All work loops were measured at 5% total strain. All loops from *Hippocampus* show positive work (loops are traversed counter-clockwise; the muscle is generating force while it is shortening in length), whereas the loops for the two highest frequencies in *Syngnathus* show negative work (loops are traversed clockwise; the muscle is generating force while it is being forced to lengthen). Thick regions of the loops indicate the period of stimulation.

all strains. Pipefish muscle was able to generate positive work at longer strains than seahorse muscle: At 15% strain, seahorse muscle produced negative work at all frequencies tested, whereas pipefish muscle produced positive work at all but the two highest frequencies (Fig. 7).

The graphs of average power output at the different frequency + strain combinations have the same general shape as those for work per cycle, with an important difference. Power output does not monotonically decrease with increasing cycle frequency. In fact, power production is maximal at an intermediate frequency (30 Hz in seahorse, 20 Hz in pipefish; Figs. 8,10). This is due to power output being simply the product of cycle frequency and work per cycle: work per cycle declines, but for a time the increasing frequency outweighs this, and power output rises. However, at some point, the work per cycle declines to the point that even very high frequencies cannot counteract this effect, and power output then declines as well (Fig. 10).

The dorsal fin muscles of *Hippocampus* and *Syngnathus* were statistically compared by a three-way ANOVA at the two frequencies (20 Hz and 30 Hz) and four strains (2.5%, 5%, 10%, and 15%) for which data was recorded in both species. Interestingly, there was not a significant effect of species on either work per cycle (Table 2) or power output (Table 3). However, both work and power output showed significant effects of frequency, strain, and the interactions of species*strain and frequency*strain (all with $P < 0.0001$; Tables 2,3). These results indicate that even within the restricted range used in this analysis, both work and power output differ significantly at different strains and frequencies. The significant species*strain interaction term indicates that the seahorse and pipefish are responding differently to the strain levels tested, which is evident from Figs. 9 and 10. Finally, the significant frequency*strain interaction indicates that the relationship between cycling frequency and strain level is complex, as discussed above. It must be pointed out that the lack of a significant species difference in these ANOVAs is somewhat misleading, as the frequencies that overlapped were very limited. Pipefish muscle was not able to generate any positive work at high frequencies, whereas seahorse muscle still performed positive work at oscillation frequencies as high as 50 Hz.

Temperature effects on muscle mechanics

Temperature exerts a significant effect on the ability of pipefish dorsal fin muscle to perform work. Maximum isometric stress did not differ significantly with temperature. Figure 11 summarizes the effect of temperature on work per cycle and power output. At each oscillation frequency+strain combination, work per cycle and power output at 20°C is significantly higher

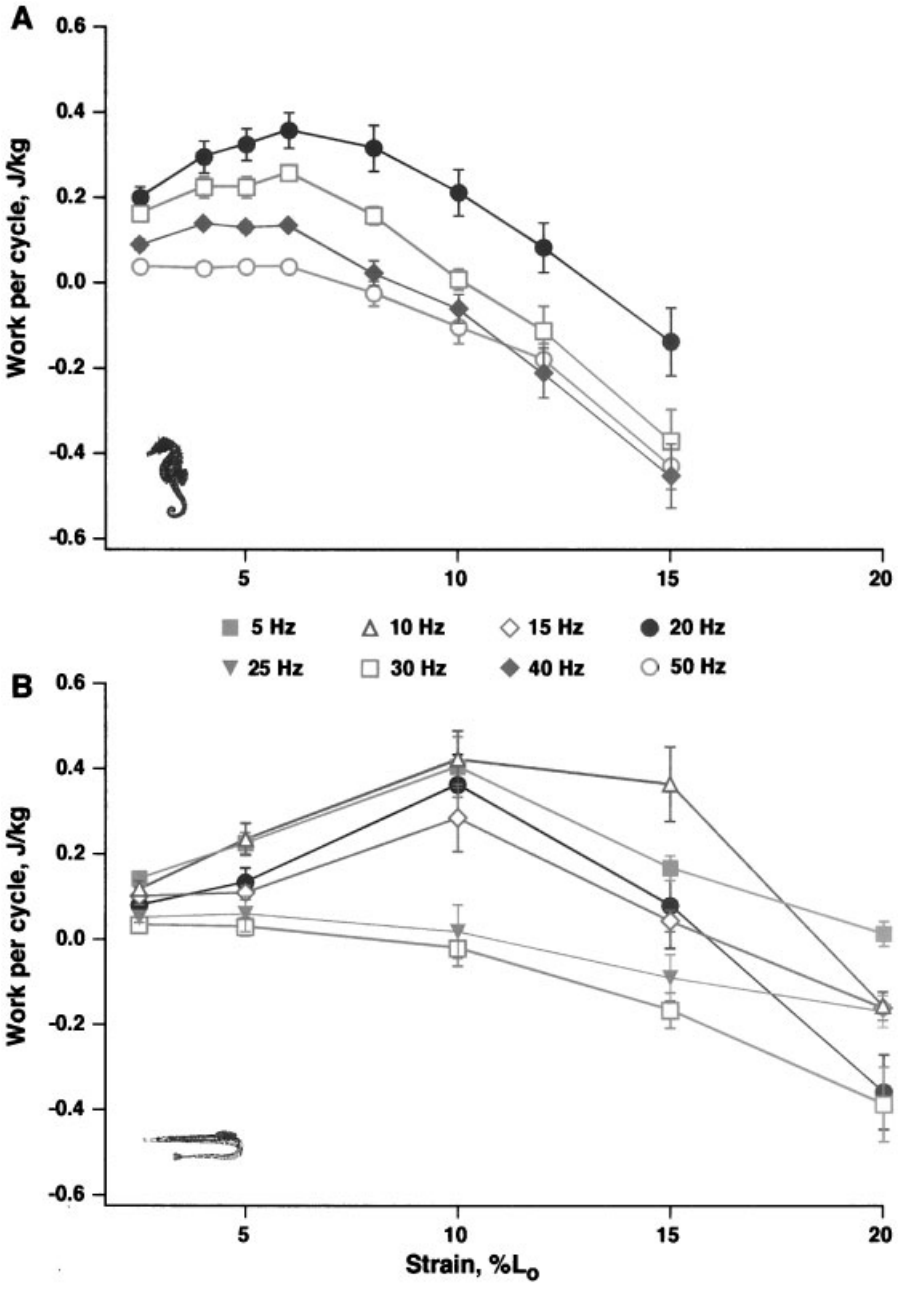

Fig. 7. Average values of work per cycle at different frequencies and strains in *Hippocampus* (**A**) and *Syngnathus* (**B**). Error bars are standard errors; some of the error bars are completely hidden by their respective symbols. Different frequencies are represented by different colored symbols and lines. Filled brown square, 5 Hz; open blue triangle, 10 Hz; open teal diamond, 15 Hz; filled black circle, 20 Hz; filled grey inverted triangle, 25 Hz; open red square, 30 Hz; filled purple diamond, 40 Hz; open green circle, 50 Hz.

(as determined by single-factor ANOVA) than at 10°C (Table 4). Q_{10} values are dependent upon the frequency+strain combination being considered, ranging from just over two at 5 Hz/2.5% strain to just under four at 5% strain (Table 4). Due to the different responses to temperature of the muscle at 10% strain (increase in work and power at 20°C, but decrease at 10°C), Q_{10} values were not calculated for this strain.

DISCUSSION

Comparison of seahorse to pipefish dorsal fin muscle

While both *Hippocampus* and *Syngnathus* use high-frequency oscillations of the dorsal fin as their primary means of movement, the dorsal fin muscles from the two species showed significant

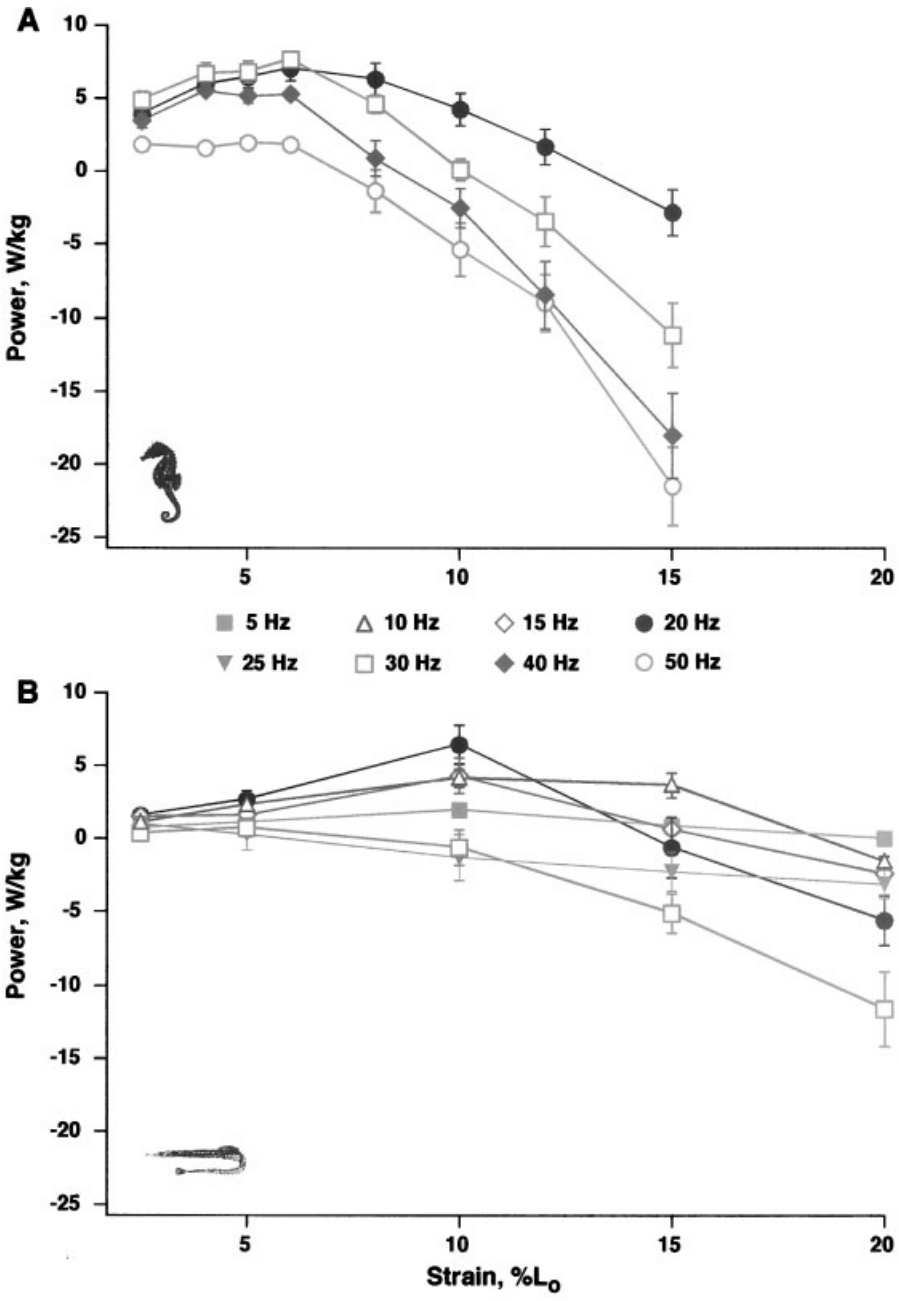

Fig. 8. Average values of power output at different frequencies and strains in *Hippocampus* (**A**) and *Syngnathus* (**B**). Error bars are standard errors; some of the error bars are completely hidden by their respective symbols. Different frequencies are represented by different colored symbols and lines. Filled brown square, 5 Hz; open blue triangle, 10 Hz; open teal diamond, 15 Hz; filled black circle, 20 Hz; filled grey inverted triangle, 25 Hz; open red square, 30 Hz; filled purple diamond, 40 Hz; open green circle, 50 Hz.

differences in several areas. Seahorse dorsal fin muscle bundles are significantly longer than those of pipefish (Table 1), while pipefish have longer dorsal fins with higher numbers of fin rays (and hence muscle slips; Fig. 1). Seahorses have noticeably deeper bodies than pipefish, with a large ventral ''belly,'' as well as an elaboration of scales into spines all over the body. It may be that the greater length of the dorsal fin muscle slips in seahorses is simply due to the greater distance between the vertebral column and the dorsal surface, rather than having specific functional significance. Maximum twitch and tetanic stress are significantly higher in *Hippocampus* dorsal fin muscle than in *Syngnathus*; mean twitch stress is nearly 2.5 times higher, while mean tetanic stress shows less of a difference, being 1.6 times higher in the seahorse. Twitch-tetanus ratio was 0.69 in seahorse and 0.45 in pipefish. Time to maximum force was also significantly shorter in *Hippocam-*

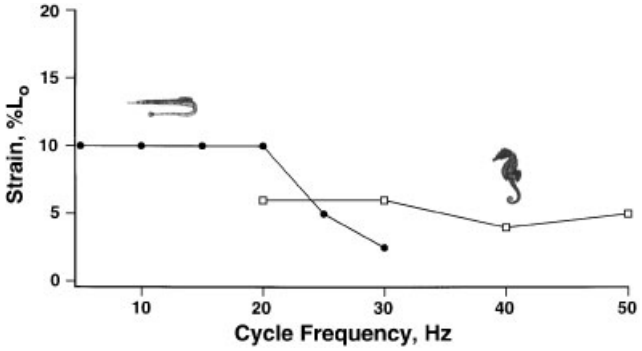

Fig. 9. Strain at which both work and power production are maximal for *Syngnathus* (filled circles) and *Hippocampus* (open squares) across a range of frequencies.

pus than in *Syngnathus* for both twitch and tetanus (Table 1), which is likely correlated to the higher in vivo contraction frequencies in the seahorse.

At the same cycling frequencies, seahorse and pipefish dorsal fin muscle generated similar amounts of work and power output (nonsignificant by ANOVA; Tables 2,3). However, work and power differed significantly with frequency and strain (Tables 2,3). Additionally, *Hippocampus* and *Syngnathus* responded differently to strain (significant species*strain interaction, Tables 2,3). Pipefish produced maximum work per cycle at longer strains than seahorse over much of the frequency range tested (10% versus 6%; Figs. 7,9). Because the L_o of pipefish dorsal fin muscle is considerably shorter than that of the seahorse, when the percent strains are converted to absolute shortening distances, the optimal distances are similar, on the order of 0.2–0.3 mm in both species. This may be of functional significance, in that the magnitude of lateral deflection of the fin rays is dependent on the absolute amount of shortening in the muscle. Similar absolute muscle shortening would thus be predicted to produce similar angular deflection of the fin rays. Though there was not a significant difference attributable to species in the ANOVA, it must be pointed out that there is nonetheless a real difference in the performance capabilities of seahorse dorsal fin muscle relative to pipefish, as *Hippocampus* was able to produce positive work and power at high cycling frequencies (>30 Hz) where *Syngnathus* dorsal fin muscle only produced negative work. Negative work values indicate that the servomotor is doing work on the muscle, and hence that the muscle is unable to contract fast enough to keep up with the servomotor.

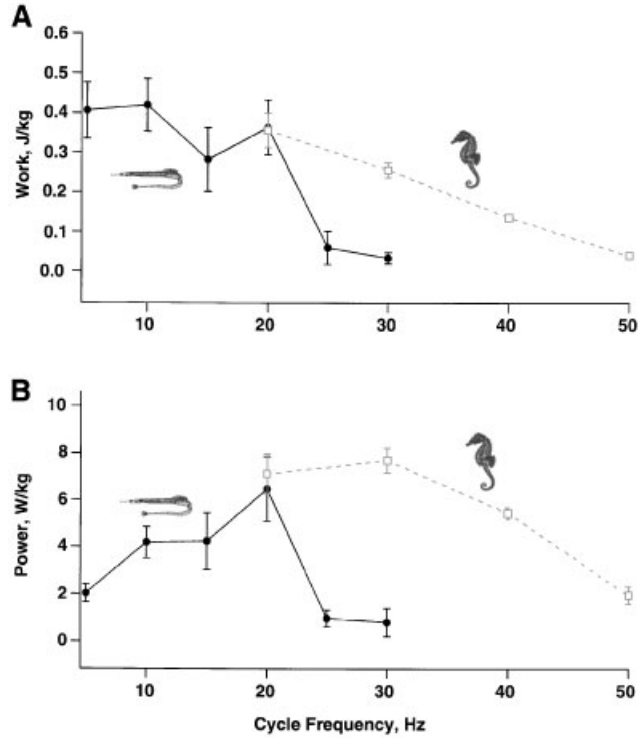

Fig. 10. Mean maximum work (**A**) and power output (**B**) at different frequencies for *Syngnathus* (filled black circles) and *Hippocampus* (open grey squares), irrespective of strain. Error bars are standard errors of the mean; some of the error bars are completely hidden by their respective symbols.

TABLE 2. ANOVA results for work per cycle (in J/kg) of the dorsal fin muscles of H. hudsonius and S. fuscus at two frequencies and four strains

Effect	F-value	*P*-value
Species (*df*=1)	0.697	0.405
Frequency (*df*=1)	69.481	<0.0001
Strain (*df*=3)	55.101	<0.0001
Species*Strain (*df*=3)	20.553	<0.0001
Frequency*Strain (*df*=3)	7.860	<0.0001

TABLE 3. ANOVA results for power output (in W/kg) of the dorsal fin muscles of H. hudsonius and S. fuscus at two frequencies and four strains

Effect	F-value	*P*-value
Species (*df*=1)	1.259	0.263
Frequency (*df*=1)	55.003	<0.0001
Strain (*df*=3)	67.655	<0.0001
Species*Strain (*df*=3)	23.137	<0.0001
Frequency*Strain (*df*=3)	15.739	<0.0001

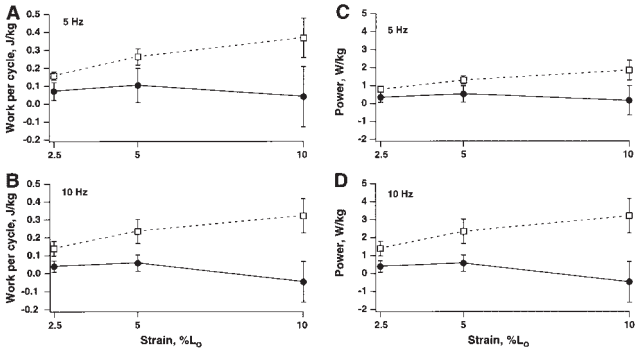

Fig. 11. Temperature effects on work (**A**, **B**) and power production (**C**, **D**) in *Syngnathus* at 2.5%, 5%, and 10% L_o strain. Filled circles, 10°C; open squares, 20°C. (A, C) 5 Hz. (B, D) 10 Hz. Error bars are standard deviations.

Comparisons to other studies

An unusual feature of the tetanic contraction for both *Hippocampus* and *Syngnathus* is the ''sag'' from the initial peak of force to the lower plateau that is maintained for the duration of stimulation (Fig. 5). This was observed in every preparation tested for seahorses and pipefish, but not for salamander muscle tested in the same experimental setup (Ashley-Ross and Barker, unpublished data), so it does not appear to be an artifact of the apparatus used. According to Bergman ('64a), the tetanic force in dorsal fin muscle of *H. hudsonius* does not show a similar decline, though the experimental preparation used in that study was quite different from that used here. Bergman mounted the dorsal fin horizontally and tied his force transducer to the distal end of the fin rays (which acted as a long lever arm). Since the fin rays will bend along their long axis, it is likely that Bergman's ('64a) arrangement acted to dampen an initial peak of force before the plateau. In the preparation used here, the tissues in series with the force transducer are the fin rays, tendons of insertion, and the dorsal fin muscles themselves. It is at present unclear what is responsible for the sag; it seems unlikely to be due to ''give'' in one of these tissues, as the sag was visible in all of the tetanic contractions, not just the first (one would expect the tissue to ''give'' once and then be stable). It may represent very fast relaxation of some muscle fibers; however, this remains to be tested experimentally. Functionally, the sag would appear to be of little consequence for the seahorse or pipefish. Patterns of dorsal fin muscle activation are unknown, but it is unlikely that long tetanic contractions occur during normal in vivo operation. At contraction frequencies resembling those in vivo, the entire strain cycle would have taken place before the plateau region of the trace had been reached. Thus, the force developed by the muscle is likely to resemble the initial peak of force, rather than the maintained plateau force.

TABLE 4. Effects of temperature on muscle mechanics in S. fuscus[1]

	10°C	20°C	Q_{10}	F-value	*P*-value
Isometric tetanic stress (N/m^2)	74.29 (41.75)	111.5 (48.72)	n/a	1.888	0.18
Work (J/kg)				133.253	<0.0001
5 Hz					
2.5%	0.074 (0.050)	0.16 (0.024)	2.18		
5%	0.10 (0.095)	0.27 (0.044)	2.54		
10%	0.041 (0.17)	0.37 (0.11)	n/a		
10 Hz					
2.5%	0.042 (0.034)	0.14 (0.043)	3.28		
5%	0.061 (0.047)	0.24 (0.069)	3.91		
10%	−0.047 (0.11)	0.32 (0.097)	n/a		
Power (W/kg)				117.975	<0.0001
5 Hz					
2.5%	0.37 (0.25)	0.80 (0.12)	2.18		
5%	0.52 (0.48)	1.33 (0.22)	2.54		
10%	0.20 (0.83)	1.85 (0.55)	n/a		
10 Hz					
2.5%	0.42 (0.34)	1.39 (0.43)	3.28		
5%	0.61 (0.47)	2.38 (0.69)	3.91		
10%	−0.47 (1.13)	3.23 (0.97)	n/a		

[1]Work and power were measured at two cycling frequencies (5 and 10 Hz) and three strains (2.5, 5, and 10 % L_o). Values for parameters are mean (SD).

TABLE 5. Comparative values of isometric parameters, work, and power output from representative vertebrate skeletal muscles

Muscle	Temperature (°C)	Max isometric stress (kN/m^2)	Time to peak twitch (ms)	Max work per cycle (J/kg)	Max power output (W/kg)	Reference
Hippocampus dorsal fin	20	176	19	0.36 [20 Hz]	7.71 [30 Hz]	This study
Syngnathus dorsal fin	20	112	22	0.42 [10 Hz]	6.48 [20 Hz]	This study
Dogfish white myotome	12	241[2]			120 [5 Hz]	(Curtin and Woledge,'96)
Stenotomus chrysops red myotome	20	183[3]		10.9 [5 Hz]	27.9 [5 Hz]	(Rome and Swank,'92)
Thunnus albacares slow fibers	20		110		6.5 [4 Hz]	(Altringham and Block,'97)
Sarda chiliensis slow fibers	20		100		11 [5 Hz]	(Altringham and Block,'97)
Dipsosaurus dorsalis iliofibularis	22	188[1]	39	7.6 [5.9 Hz]	42.6 [5.9 Hz]	(Swoap et al.,'93)
	42		11	7.8 [20.1 Hz]	153.7 [20.1 Hz]	
Toadfish white myotome	15	228	79			(Rome et al.,'99)
Toadfish swimbladder muscle	15	56	6 (25°C)			(Rome et al.,'99)
Frog sartorius	20	350		15 [4 Hz]	60 [4 Hz]	(Stevens,'96)
Mouse soleus	35	224	22	4.9 [5 Hz]	34.0 [5 Hz]	(James et al.,'95)
Mouse extensor digitorum longus	35	233	10	11.8 [10 Hz]	107.2 [10 Hz]	(James et al.,'95)

[1]Value taken from (Marsh and Bennett,'85), measured at 25°C.
[2]Value taken from (Curtin and Woledge,'88).
[3]Value taken from (Rome et al.,'92).

Time to peak twitch tension in *Hippocampus* measured in this study (19 ms; Table 1) is close to the value given by Bergman ('64a), who reported a mean of 13 ms to reach peak tension. The slower time in the present study is likely due to measurements being made at 20°C in this study versus 25°C in Bergman's ('64a) work. Values reported by Bergman ('64a) for twitch tension cannot be compared to those given here, as information regarding muscle dimensions was not reported, and the ''lever arm'' arrangement used is not comparable to the direct measurements used here. The seahorse and pipefish dorsal fin muscles show a slower twitch rise time than individual fast fibers from Pacific sand dab dorsal fin muscle (Gilly and Aladjem, '87), which attain peak tension in approximately 10 ms. However, the fast fibers examined by Gilly and Aladjem ('87) were determined by histochemical staining to be fast glycolytic (white) fibers with very little oxidative capacity (Franzini-Armstrong et al., '87). This finding contrasts with seahorse dorsal fin muscle, which has been shown to stain as highly oxidative (Hale, '96).

The maximum tetanic stress in *Hippocampus* and *Syngnathus* dorsal fin muscle is smaller than that measured in locomotor muscle from other vertebrate species, which usually average 200–300 kN/m^2 (Table 5, Josephson, '93). Myofibrils occupy only 61% of the fiber volume in seahorse dorsal fin muscle (Smith et al., '88); when corrected for myofibrillar cross-sectional area, maximum tetanic stress is approximately 290 kN/m^2 in *Hippocampus*. Ultrastructure of pipefish dorsal fin muscle has not been examined, but if the myofibrils comprise the same proportion of cell volume as in the seahorse, then the maximum tetanic stress in *Syngnathus* would be approximately 180 kN/m^2. The estimates for maximum tetanic stress when corrected for myofibrillar volume are thus similar to those reported for other locomotor muscles.

The time to peak twitch force for seahorse and pipefish dorsal fin muscle is shorter than other locomotor muscles measured at the same temperature (Table 5). A faster rate of rise in force is expected due to the high in vivo cycling frequencies of dorsal fin muscles in the two species. However, neither pipefish nor seahorse dorsal fin muscle can match the rapidity of the twitch kinetics of the sound-producing swimbladder muscle of toadfish, with a time to peak twitch force of $\approx$6 ms (Table 5; Rome et al., '96). The swimbladder muscle contracts and relaxes extremely quickly, primarily due to an unusually high crossbridge dissociation rate (Rome et al., '99) that

has the side effect of limiting the muscle to low force production (Table 5) due to low numbers of attached crossbridges. For twitch contraction time and isometric stress, the dorsal fin muscles of *Hippocampus* and *Syngnathus* are intermediate between toadfish swimbladder muscle and other locomotor muscles (Table 5).

Comparison of values for work and power output of dorsal fin muscle from *Hippocampus* and *Syngnathus* to those of other muscles is difficult due to the paucity of data from comparable cycling frequencies. Nonetheless, some conclusions are possible. Maximum work per cycle in both species is an order of magnitude lower than the values reported for other vertebrate species. At similar frequencies but higher temperatures, lizard iliofibularis and mouse extensor digitorum longus (EDL) muscles produce over 20 × the work per cycle of the dorsal fin muscles studied here (Table 5). Using the Q_{10} value for 10 Hz, 5% strain for *Syngnathus*, raising its dorsal fin muscle to the same temperature as the mouse EDL would result in net work per cycle of 3.24 J/kg, still less than one-third the value of mouse muscle.

At comparable temperatures, frequencies giving optimal work and power production in other vertebrate locomotor muscles are considerably lower than the optimal frequencies for seahorse and pipefish dorsal fin muscles. Due to the higher preferred cycling frequencies, maximum power output values for *Hippocampus* and *Syngnathus* are closer to those reported for slow fibers in other fish, but much lower than the values for white (anaerobic) myotomal muscle (Table 5). Seahorse dorsal fin muscle is highly aerobic (Bergman, '64b; Smith et al., '88) and is classified as oxidative muscle by histochemical staining (Hale, '96). However, it operates at higher frequencies than other highly oxidative muscles. In fact, seahorse and pipefish dorsal fin muscles are able to generate positive work at cycling frequencies higher than those that have been recorded for myotomal muscle (red or white) from other fish.

Why are values for work per cycle so low in *Hippocampus* and *Syngnathus*? The high cycling frequencies likely explain much of this result. The time taken up by the cycle is so short that the muscle would have to generate extraordinarily high forces to produce large values of work per cycle. Even at 20 Hz (the lowest frequency tested for the seahorse), the entire lengthen-shorten-relengthen cycle takes place so rapidly (entire cycle in 50 ms) that the maximum isometric force does not have time to develop before the muscle begins shortening at 25% of the way through the cycle (compare time to maximum twitch force in Table 1). Force falls rapidly during shortening and is very low during the re-stretch to L_o (Fig. 6). If contraction and relaxation of the dorsal fin muscle followed the time course of an isometric twitch, then the muscle would still be generating force at the end of the cycle (about half way through relaxation; see Fig. 5). However, it is well-known that muscle force and shortening velocity vary inversely (reviewed in Josephson, '93). The more rapidly a muscle shortens, the less force it is able to sustain. At the frequency+strain combinations used here, shortening velocities range from 0.125 muscle lengths/sec (pipefish at 5 Hz, 2.5% strain) to 7.5 lengths/sec (seahorse at 50 Hz, 15% strain). At the higher frequencies and larger strains, shortening velocity is likewise high, and the force-velocity relationship results in the force developed during shortening being low. Thus, low values for work per cycle are an expected consequence of the high muscle shortening velocities resulting from the high cycling frequencies. Indeed, at the higher frequencies tested for seahorse (40 Hz and 50 Hz), strain above 10% resulted in negative work, indicating that the muscle was unable to keep pace with the servomotor. However, work per cycle was also low at low cycling frequencies, where the shortening velocity of the muscle would be expected to be in a range of the force-velocity curve where force would still be high. Small amounts of work at low cycling frequencies, and the very low force during re-stretch at all cycling frequencies, may indicate that shortening (work-dependent) deactivation (Josephson and Stokes, '99) is occurring in the dorsal fin muscle. Work-dependent deactivation is an important property of muscles that perform cyclic contractions, particularly at high frequency, as it allows the muscle to be re-lengthened by antagonist muscles without generating negative work that would impede movement (Josephson, '99; Josephson and Stokes, '99). While shortening deactivation is important in allowing the dorsal fin muscles to function at high frequencies, it reduces the force maintained during the cycle, and hence the work performed.

Relatively low power output by the muscles, combined with inefficient transfer of momentum to the surrounding water (Blake, '80), restricts seahorses and pipefish to slow swimming speeds. However, both species have little need to move rapidly, relying on crypsis to avoid predation. The

dorsal fin muscles are well-suited to this task: they beat the fin back and forth so rapidly that its movement is above the frequency for flicker fusion in humans, and likely for their natural predators as well (Blake, '76). The fin is thus rendered invisible, and the swimming animal appears to be nothing more than a drifting bit of eelgrass, kelp, or coral.

ACKNOWLEDGMENTS

I thank Robert Josephson for teaching me how to measure muscle work, for many valuable discussions on muscle, and for critical comments on the manuscript. William Conner, Herman Eure, and Wayne Silver also provided critical comments on the manuscript.

LITERATURE CITED

Altringham JD, Block BA. 1997. Why do tuna maintain elevated slow muscle temperatures? Power output of muscle isolated from endothermic and ectothermic fish. J Exp Biol 200:2617–2627.

Bass AH. 1990. Sounds from the intertidal zone— vocalizing fish. Bioscience 40:249–258.

Bass AH, Marchaterre MA. 1989. Sound-generating (sonic) motor system in a teleost fish *(Porichthys notatus)*— sexual polymorphism in the ultrastructure of myofibrils. J Comp Neurol 286:141–153.

Bergman RA. 1964a. Mechanical properties of the dorsal fin musculature of the marine teleost, *Hippocampus hudsonius*. Bull Johns Hopkins Hosp 114:344–353.

Bergman RA. 1964b. The structure of the dorsal fin musculature of the marine teleosts, *Hippocampus hudsonius* and *H. zosterae*. Bull Johns Hopkins Hosp 114:325–343.

Blake RW. 1976. On seahorse locomotion. J Mar Biol Assoc UK 56:939–949.

Blake RW. 1980. Undulatory median fin propulsion of two teleosts with different modes of life. Can J Zool 58:2116–2119.

Breder CM, Edgerton HE. 1942. An analysis of the locomotion of the seahorse, *Hippocampus*, by means of high speed cinematography. Ann N Y Acad Sci 43:145–172.

Clark AW, Schultz E. 1980. Rattlesnake shaker muscle. II. Fine structure. Tissue Cell 12:335–351.

Close RL, Luff AR. 1974. Dynamic properties of inferior rectus muscle of the rat. J Physiol Lond 236:259–270.

Consi TR, Seifert PA, Triantafyllou MS, Edelman ER. 2001. The dorsal fin engine of the seahorse *(Hippocampus sp.)*. J Morphol 248:80–97.

Cooper S, Eccles J. 1930. The isometric responses of mammalian muscles. J Physiol Lond 69:377–385.

Curtin N, Woledge R. 1996. Power at the expense of efficiency in contraction of white muscle fibres from dogfish Scyliorhinus canicula. J Exp Biol 199:593–601.

Curtin NA, Woledge RC. 1988. Power output and force-velocity relationship of live fibers from white myotomal muscle of the dogfish, *Scyliorhinus canicula*. J Exp Biol 140:187–197.

Fawcett DW, Revel JP. 1961. The sarcoplasmic reticulum of a fast-acting fish muscle. J Biophys Biochem Cytol Suppl 10:89.

Fine ML. 1989. Embryonic, larval and adult development of the sonic neuromuscular system in the oyster toadfish. Brain Behav Evol 34:13–24.

Fine ML, Burns NM, Harris TM. 1990. Ontogeny and sexual dimorphism of sonic muscle in the oyster toadfish. Can J Zool 68:1374–1381.

Franzini-Armstrong C, Gilly WF, Aladjem E, Appelt D. 1987. Golgi stain identifies three types of fibres in fish muscle. J Muscle Res Cell Motil 8:418–427.

Geerlink PJ, Videler JJ. 1974. Joints and muscles of the dorsal fin of *Tilapia nilotica* L. (Fam. Cichlidae). Neth J Zool 24:279–290.

Gilly WF, Aladjem E. 1987. Physiological properties of three muscle fibre types controlling dorsal fin movements in a flatfish, *Citharichthys sordidus*. J Muscle Res Cell Motil 8:407–417.

Greenewalt CH. 1975. The flight of birds: the significant dimensions, their departure from the requirements for dimensional similarity, and the effect on flight aerodynamics of that departure. Trans Am Phil Soc 65:1–67.

Hale ME. 1996. Functional morphology of ventral tail bending and prehensile abilities of the seahorse, *Hippocampus kuda*. J Morphol 227:51–65.

James RS, Altringham JD, Goldspink DF. 1995. The mechanical properties of fast and slow skeletal muscles of the mouse in relation to their locomotory function. J Exp Biol 198:491–502.

Josephson RK. 1985. Mechanical power output from striated muscle during cyclic contraction. J Exp Biol 114:493–512.

Josephson RK. 1993. Contraction dynamics and power output of skeletal muscle. Annu Rev Physiol 55:527–546.

Josephson RK. 1999. Dissecting muscle power output. J Exp Biol 202 Pt 23:3369–3375.

Josephson RK, Stokes DR. 1999. Work-dependent deactivation of a crustacean muscle. J Exp Biol 202:2551–2565.

Knapp AG, Dowling JE. 1987. Dopamine enhances excitatory amino acid-gated conductances in cultured retinal horizontal cells. Nature 325:437–439.

Lindsey CC. 1978. Form, function, and locomotory habits in fish. In: Hoar WS, Randall DJ, editors. Fish physiology. New York: Academic Press. p 1–100.

Marsh RL, Bennett AF. 1985. Thermal dependence of isotonic contractile properties of the skeletal muscle and sprint performance of the lizard *Dipsosaurus dorsalis*. J Comp Physiol [B] 155:541–555.

Revel JP. 1962. The sarcoplasmic reticulum of the bat cricothyroid muscle. J Cell Biol 12:571.

Rome LC, Swank D. 1992. The influence of temperature on power output of scup red muscle during cyclical length changes. J Exp Biol 171:261–281.

Rome LC, Sosnicki A, Choi IH. 1992. The influence of temperature on muscle function in the fast swimming scup. II. The mechanics of red muscle. J Exp Biol 163:281–295.

Rome LC, Syme DA, Hollingworth S, Lindstedt SL, Baylor SM. 1996. The whistle and the rattle: the design of sound producing muscles. Proc Natl Acad Sci U S A 93:8095–8100.

Rome LC, Cook C, Syme DA, Connaughton MA, Ashley-Ross M, Klimov A, Tikunov B, Goldman YE. 1999. Trading force for speed: why superfast crossbridge kinetics leads to superlow forces. Proc Natl Acad Sci U S A 96:5826–5831.

Schultz E, Clark AW, Suzuki A, Cassens RG. 1980. Rattlesnake shaker muscle. I. A light microscopic and histochemical study. Tissue Cell 12:323–334.

Smith DS, Morales M, Del Castillo J. 1988. Dorsal fin and myotome muscle of the sea horse, *Hippocampus*. Puerto Rico Health Sci J 7:183–184.

Stevens ED. 1996. The pattern of stimulation influences the amount of oscillatory work done by frog muscle. J Physiol Cambridge 494:279–285.

Suarez RK, Lighton JRB, Brown GS, Mathieu-Costello O. 1991. Mitochondrial respiration in hummingbird flight muscles. Proc Natl Acad Sci U S A 88:4870–4873.

Swoap SJ, Johnson TP, Josephson RK, Bennett AF. 1993. Temperature, muscle power output and limitations on burst locomotor performance of the lizard *Dipsosaurus dorsalis*. J Exp Biol 174:185–197.

Videler J. 1993. Fish swimming. London: Chapman and ;Hall.

Webb PW. 1982. Locomotor patterns in the evolution of actinopterygian fishes. Amer Zool 22:329–342.

Winterbottom R. 1974. A descriptive synonymy of the striated muscles of the teleostei. Proc Acad Nat Sci Philadelphia 125:225–317.

Withers PC. 1992. Comparative animal physiology. Fort Worth, TX: Saunders College Publishing.